

DETERMINATION OF PROPAGATION CONSTANTS AND MATERIAL DATA FROM WAVEGUIDE MEASUREMENTS

D. Sjöberg

Department of Electrical and Information Technology
Lund University
P. O. Box 118, 221 00 Lund, Sweden

Abstract—This paper presents an analysis with the aim of characterizing the electromagnetic properties of an arbitrary linear, bianisotropic material inside a metallic waveguide. The result is that if the number of propagating modes is the same inside and outside the material under test, it is possible to determine the propagation constants of the modes inside the material by using scattering data from two samples with different lengths. Some information can also be obtained on the cross-sectional shape of the modes, but it remains an open question if this information can be used to characterize the material. The method is illustrated by numerical examples, determining the complex permittivity for lossy isotropic and anisotropic materials.

1. INTRODUCTION

In order to obtain a well controlled environment for making measurements of electromagnetic properties, it is common to do the measurements in a metallic cavity or waveguide. The geometrical constraints of the waveguide walls impose dispersive characteristics on the propagation of electromagnetic waves, i.e., the wavelength of the propagating wave depends on frequency in a nonlinear manner. In order to correctly interpret the measurements, it is necessary to provide a suitable characterization of the waves inside the waveguide. This is well known for isotropic materials [2, 3, 12, 20], bi-isotropic (chiral) materials [9, 17], and even anisotropic materials where an optical axis is along the waveguide axis [1, 10, 15, 16], but for general bianisotropic

Corresponding author: D. Sjöberg (daniel.sjoberg@eit.lth.se).

media with arbitrary axes there are so far very few results available. In principle, an optimization approach as in [12] and [16] can be designed, where the material parameters are found by minimizing the distance between measured and simulated S -parameters. However, this method is typically plagued by non-uniqueness and similar numerical issues, and we seek a more direct method, providing physical insight to the problem.

We present in this paper a partial solution to an inverse scattering problem in a waveguide geometry. It is partial in the respect that the primary information to be determined is the propagation constants of the propagating modes in the material. The subsequent problem is to extract information on the material from the propagation constants, which we show how to solve for some special cases, but the general case is still open. The direct problem is solved by defining modes in an arbitrary linear material. This solution helps us define an N -port model of the scattering problem, which is then utilized in the inverse problem. Most of the references mentioned so far only treats the single-mode case, but the formalism in this paper is ready for an arbitrary number of modes. However, in practical applications the single-mode case is usually preferable since it is difficult to measure higher order modes.

A general formalism for anisotropic waveguides was presented in a series of papers in the late fifties [5–8], but they have had surprisingly few followers. The bianisotropic case is treated by [21] and [4]. In these papers, the fundamental eigenvalue problem defining the modes in a bianisotropic material is defined and explored for general orthogonality properties, but it is not applied to a scattering problem. There is a scattering formalism for discontinuities in [21], but it is rather vague and there is also some confusion about propagating and evanescent modes in this paper. This is better accounted for in [4], but the formalism is only used to study the excitation of modes, not in a scattering problem. In [22, 23], a coupled-mode analysis is performed for bianisotropic waveguides, i.e., the fields inside the material are expanded in terms of modes corresponding to an isotropic material. The scattering problem is not treated here either, but there are some graphs of dispersion relations in [22].

In this paper, we use an eigenvalue problem of the form used in [4, 7, 21] to define modes propagating in a metallic waveguide filled with a bianisotropic material. The approach is related to similar spectral decompositions used in homogenization theory [18, 19], where the boundary conditions of the waveguide are replaced by periodic boundary conditions. Using these modes, we define an expansion of the electromagnetic field, which is then used in a mode-matching analysis

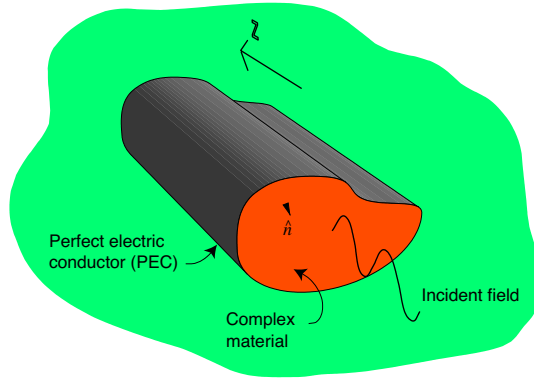


Figure 1. Geometry of the waveguide. The “complex” material may be anisotropic, bianisotropic, lossy, etc, but has to be linear.

of the scattering problem. In order to deduce the general properties of this formulation, the quasi-orthogonality results from [4, 8, 21] are used extensively, and they are repeated in Section 4.

The paper is organized as follows. Some preliminary notions are made in Section 2, and in Section 3, we illustrate what makes the isotropic case so simple, namely that it is possible to define an eigenvalue problem independent of both frequency and propagation constant. In Section 4, we define the general eigenproblem in terms of a first order differential equation. The forward scattering problem is treated in Section 5, and the inverse scattering problem in Section 6. The resulting algorithm is tested in a numerical example for a non-magnetic, isotropic lossy dielectric medium in Section 7, and some conclusions are given in Section 8.

2. PRELIMINARIES

We consider time-harmonic waves in a waveguide of infinite extent in the z -direction, as in Figure 1. The electromagnetic fields then satisfy (where we use SI units and time convention $e^{-i\omega t}$)

$$\nabla \times \mathbf{H} = -i\omega \mathbf{D} = -i\omega(\epsilon \mathbf{E} + \boldsymbol{\xi} \mathbf{H}) \quad (1)$$

$$\nabla \times \mathbf{E} = i\omega \mathbf{B} = i\omega(\boldsymbol{\mu} \mathbf{H} + \boldsymbol{\zeta} \mathbf{E}) \quad (2)$$

for $(x, y) \in \Omega$ and z arbitrary, with the boundary conditions $\hat{\mathbf{n}} \times \mathbf{E} = \mathbf{0}$ and $\hat{\mathbf{n}} \times \mathbf{H} = \mathbf{J}_S$, where \mathbf{J}_S is the surface current and $\hat{\mathbf{n}}$ is the unit normal pointing into the region Ω . The surface current is usually unknown, and the boundary condition $\hat{\mathbf{n}} \times \mathbf{H} = \mathbf{J}_S$ should be

considered as a means of determining \mathbf{J}_S , not as a restrictive condition on \mathbf{H} . The PEC (Perfect Electric Conductor) condition $\hat{\mathbf{n}} \times \mathbf{E} = \mathbf{0}$ is sufficient to calculate the fields. In the case of a lossy metallic wall, this condition can be replaced by an impedance boundary condition.

In the typical case when the material parameters do not depend on z , we consider fields with an exponential dependence on z ,

$$\begin{pmatrix} \mathbf{E}(x, y, z) \\ \mathbf{H}(x, y, z) \end{pmatrix} = \begin{pmatrix} \mathbf{E}(x, y) \\ \mathbf{H}(x, y) \end{pmatrix} e^{\gamma z} \quad (3)$$

where $\gamma = \alpha + i\beta$ is a complex number. Maxwell's equations can then be written (where $\nabla_t = \hat{\mathbf{x}}\partial_x + \hat{\mathbf{y}}\partial_y$)

$$\begin{pmatrix} \mathbf{0} & -(\nabla_t + \gamma\hat{\mathbf{z}}) \times \\ (\nabla_t + \gamma\hat{\mathbf{z}}) \times & \mathbf{0} \end{pmatrix} \begin{pmatrix} \mathbf{E} \\ \mathbf{H} \end{pmatrix} = i\omega \underbrace{\begin{pmatrix} \epsilon & \xi \\ \zeta & \mu \end{pmatrix}}_{=\mathbf{M}} \begin{pmatrix} \mathbf{E} \\ \mathbf{H} \end{pmatrix} \quad (4)$$

For propagating waves in a lossless waveguide, we have $\gamma = i\beta$. Lossless media are characterized by the material matrix \mathbf{M} being a hermitian symmetric positive definite matrix, i.e., $\mathbf{M}^H = \mathbf{M}$ and $\mathbf{e}^H \mathbf{M} \mathbf{e} \geq \theta |\mathbf{e}|^2$ for some positive constant θ and all six-vectors $\mathbf{e} = [\mathbf{E}, \mathbf{H}]^T$. Under these conditions, (4) is a well posed eigenvalue problem for a self-adjoint operator for each fixed β , where ω is the eigenvalue. A detailed account in the homogenization setting, where the PEC boundary condition is replaced by periodic boundary conditions, can be found in [19].

Should \mathbf{M} not be hermitian symmetric, a similar analysis of the well-posedness can be made using a singular value decomposition. Though, we shall assume that (4) defines suitable modes even in the nonhermitian case, where the typical effect is that properties such as orthogonality disappear [4]. This assumption means we consider relatively small losses, so that it makes sense to talk about wave propagation.

3. ISOTROPIC MATERIALS

Equation (4) defines the eigenvalue ω as a function of the parameter γ . To illustrate how this problem corresponds to the classical approach for isotropic waveguides, we now digress a bit to treat this special case. For isotropic materials, the first order system (4) can be written as a second order scalar equation,

$$-\nabla_t^2 u = (\omega^2 \epsilon \mu + \gamma^2) u = \lambda u \quad (5)$$

where $\nabla_t^2 = \partial_x^2 + \partial_y^2$ is the transverse Laplace operator. We see that by treating $\omega^2 \epsilon \mu + \gamma^2$ as a new eigenvalue λ , an eigenvalue problem

independent of both ω and γ can be formulated and precomputed, which provides us with dispersion relations as $\omega = \sqrt{(\lambda_n - \gamma^2)/(\epsilon\mu)}$, where λ_n depends only on the shape of the boundary. Usually two different eigenvalue problems are formulated: one for the z component of the electric field $u = E_z$ with Dirichlet conditions $u = 0$ on the boundary (TM modes), and one for the z component of the magnetic field $u = H_z$ with Neumann conditions $\hat{n} \cdot \nabla_t u = 0$ on the boundary (TE modes).

The dispersion relation $\omega = \sqrt{(\lambda_n - \gamma^2)/(\epsilon\mu)}$ immediately demonstrates the important phenomenon of a cutoff frequency. For a hollow waveguide (consisting of a simply connected region Ω enclosed by PEC walls), the smallest eigenvalue λ_0 is always positive. This means that there exists a cutoff frequency $\omega_c = \sqrt{\lambda_0}/\sqrt{\epsilon\mu}$, below which there can be no fixed frequency propagating waves corresponding to a purely imaginary propagation constant $\gamma = i\beta$, since then $-\gamma^2 = \beta^2 > 0$.

4. BIANISOTROPIC MATERIALS

It is very difficult, maybe impossible, to derive an eigenvalue problem independent of both ω and γ for a general bianisotropic material. Equation (4) can be used as an eigenvalue problem determining ω for a fixed γ , but in most practical applications it is more relevant to study a fixed frequency ω . We postulate an eigenvalue problem for the propagation constant as

$$\gamma_m \begin{pmatrix} \mathbf{0} & -\hat{z} \times \\ \hat{z} \times & \mathbf{0} \end{pmatrix} \begin{pmatrix} \mathbf{E}_m \\ \mathbf{H}_m \end{pmatrix} = \left[\begin{pmatrix} \mathbf{0} & \nabla_t \times \\ -\nabla_t \times & \mathbf{0} \end{pmatrix} + i\omega \begin{pmatrix} \epsilon & \xi \\ \zeta & \mu \end{pmatrix} \right] \begin{pmatrix} \mathbf{E}_m \\ \mathbf{H}_m \end{pmatrix} \quad (6)$$

This almost looks like an eigenvalue problem on generalized standard form, i.e., $Au = \lambda Bu$, except that the mass matrix $B = \begin{pmatrix} \mathbf{0} & -\hat{z} \times \\ \hat{z} \times & \mathbf{0} \end{pmatrix}$ is not positive definite, which is usually required. The eigenvalues of this matrix are $-1, 0, 1$, all with double multiplicity. The strict mathematical problem of showing that this problem is well posed seems to be an open issue.

The idea with this eigenvalue problem is to expand the electromagnetic field in the eigenmodes, and insert them into the z -dependent Maxwell's equations which then produces ordinary differential equations for the expansion coefficients. It then turns out that the solution is simply an expansion in these modes multiplied by exponential functions $e^{\gamma_n z}$, and the expansion coefficients can be determined from the boundary condition that the total transverse

electromagnetic field is continuous across the boundary between the surrounding medium and the material.

We now demonstrate some general properties for the solutions of the eigenproblem (6). It has already been said that a lossless material is characterized by a hermitian symmetric material matrix, $\mathbf{M} = \mathbf{M}^H$. It is convenient to have a means of characterizing the losses in a general material matrix \mathbf{M} . This is related to the anti-hermitian part, and we use the notation

$$\boldsymbol{\sigma}_M = -i\omega \frac{\mathbf{M} - \mathbf{M}^H}{2} = \frac{-i\omega}{2} \begin{pmatrix} \boldsymbol{\epsilon} - \boldsymbol{\epsilon}^H & \boldsymbol{\xi} - \boldsymbol{\xi}^H \\ \boldsymbol{\zeta} - \boldsymbol{\zeta}^H & \boldsymbol{\mu} - \boldsymbol{\mu}^H \end{pmatrix} \quad (7)$$

The hermitian symmetric matrix $\boldsymbol{\sigma}_M$ is postulated to be non-negative, since this corresponds to passive media [14]. The notation is motivated by considering the typical example of an isotropic medium with electric conductivity:

$$\mathbf{M} = \begin{pmatrix} \left(\boldsymbol{\epsilon} + \frac{\boldsymbol{\sigma}}{-i\omega} \right) \mathbf{I} & \mathbf{0} \\ \mathbf{0} & \mu \mathbf{I} \end{pmatrix} \implies \boldsymbol{\sigma}_M = \begin{pmatrix} \boldsymbol{\sigma} \mathbf{I} & \mathbf{0} \\ \mathbf{0} & \mathbf{0} \end{pmatrix} \quad (8)$$

We now sketch the derivation of the important quasi-orthogonality relation for the modes. We start by noting that

$$\begin{aligned} \begin{pmatrix} \mathbf{E}_n \\ \mathbf{H}_n \end{pmatrix}^H \begin{pmatrix} \mathbf{0} & -\hat{\mathbf{z}} \times \\ \hat{\mathbf{z}} \times & \mathbf{0} \end{pmatrix} \begin{pmatrix} \mathbf{E}_m \\ \mathbf{H}_m \end{pmatrix} &= \mathbf{E}_n^* \cdot (-\hat{\mathbf{z}} \times \mathbf{H}_m) + \mathbf{H}_n^* \cdot (\hat{\mathbf{z}} \times \mathbf{E}_m) \\ &= \hat{\mathbf{z}} \cdot (\mathbf{E}_m \times \mathbf{H}_n^* + \mathbf{E}_n^* \times \mathbf{H}_m) \end{aligned} \quad (9)$$

Multiplying Equation (6) with the (complex conjugated) solution corresponding to another eigenvalue γ_n , integrating over the cross section and integrating by parts, we obtain

$$\begin{aligned} &\gamma_m \int_{\Omega} \hat{\mathbf{z}} \cdot (\mathbf{E}_m \times \mathbf{H}_n^* + \mathbf{E}_n^* \times \mathbf{H}_m) dS \\ &= -\gamma_n^* \int_{\Omega} \hat{\mathbf{z}} \cdot (\mathbf{E}_m \times \mathbf{H}_n^* + \mathbf{E}_n^* \times \mathbf{H}_m) dS - 2 \int_{\Omega} \begin{pmatrix} \mathbf{E}_n \\ \mathbf{H}_n \end{pmatrix}^H \boldsymbol{\sigma}_M \begin{pmatrix} \mathbf{E}_m \\ \mathbf{H}_m \end{pmatrix} dS \end{aligned} \quad (10)$$

which can also be found as the result of applying the frequency domain reciprocity relation, see [11, Sec. 28.3]. Introducing the notation

$$P_{mn} = \frac{1}{2} \int_{\Omega} \hat{\mathbf{z}} \cdot (\mathbf{E}_m \times \mathbf{H}_n^* + \mathbf{E}_n^* \times \mathbf{H}_m) dS \quad (11)$$

$$Q_{mn} = \int_{\Omega} \begin{pmatrix} \mathbf{E}_n \\ \mathbf{H}_n \end{pmatrix}^H \boldsymbol{\sigma}_M \begin{pmatrix} \mathbf{E}_m \\ \mathbf{H}_m \end{pmatrix} dS \quad (12)$$

where P_{mn} represents the time average of the mutual power flow in the z direction, this implies the quasi-orthogonality relation (see also [4, 8])

$$(\gamma_m + \gamma_n^*)P_{mn} = -Q_{mn} \quad (13)$$

When $m = n$, we have $\gamma_m + \gamma_n^* = 2\text{Re}(\gamma_n)$, which can be used to characterize the different modes with respect to propagation direction as follows. A lossless waveguide is characterized by $\sigma_M = \mathbf{0}$. In this case, either $\text{Re}(\gamma_n) = \alpha_n$ is equal to zero, i.e., the mode propagates undamped with $\gamma_n = i\beta_n$, or the time average of the power flow in the z direction, P_{nn} , is zero. In a lossy waveguide, the sign of $\text{Re}(\gamma_n)$ must be the opposite of the sign of the power flow P_{nn} , since Q_{nn} is non-negative. This last property implies that we can enumerate the modes according to the signs of $\text{Re}(\gamma_n)$ and P_{nn} ,

$$n > 0 \quad \text{if} \quad \text{Re}(\gamma_n) \leq 0 \quad \text{and} \quad P_{nn} \geq 0 \quad (14)$$

$$n < 0 \quad \text{if} \quad \text{Re}(\gamma_n) \geq 0 \quad \text{and} \quad P_{nn} \leq 0 \quad (15)$$

There is no mode corresponding to $n = 0$. This splitting is unique in lossy waveguides, and can be introduced in lossless waveguides by considering the modes as limits of modes in lossy waveguides when the loss $\sigma_M \rightarrow \mathbf{0}$. We use this splitting when analyzing the scattering problems.

In lossless waveguides, the quasi-orthogonality relation (13) demonstrates that the mutual power flow P_{mn} can be non-zero only if $\gamma_m + \gamma_n^* = 0$. This is achieved when $m = n$ for propagating modes, $\gamma_n = i\beta_n$, but also for pairs of evanescent modes where $\gamma_m = \alpha$ and $\gamma_n = -\alpha$. Thus, for evanescent modes in lossless waveguides we always have $P_{nn} = 0$, but P_{-nn} may be nonzero. This condition demonstrates how evanescent modes decaying in opposite directions can couple and carry power through a structure, which is known as the tunnelling effect in quantum mechanics. These modes are called twin-conjugate modes in [4]. Even though the concept of propagating and evanescent modes can only be clearly defined in lossless media, we assume the phenomenology is present also in the case of small material losses, i.e., a finite number of modes are weakly damped (corresponding to propagating modes), and the rest are strongly damped (corresponding to evanescent modes).

5. THE FORWARD SCATTERING PROBLEM

The purpose of this section is to provide a mode-matching formulation for the forward scattering problem that can be used to solve the inverse scattering problem. We assume a scattering geometry as in Figure 2.

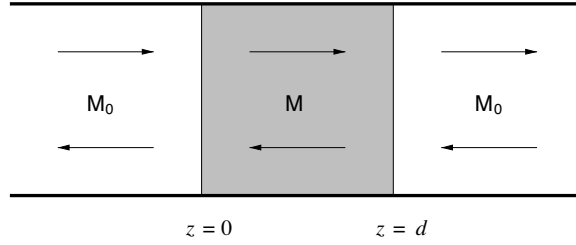


Figure 2. The scattering geometry in the waveguide. The material under test (MUT) is confined to the region $0 < z < d$ with material parameters M , and the surrounding parts of the waveguide are filled with material M_0 , usually air.

The time harmonic field amplitudes in the different regions can then be expanded as

$$\sum_{n=-N}^N A_n \begin{pmatrix} \mathbf{E}_n^0 \\ \mathbf{H}_n^0 \end{pmatrix} e^{\gamma_n^0 z} + \sum_{n < -N} A_n \begin{pmatrix} \mathbf{E}_n^0 \\ \mathbf{H}_n^0 \end{pmatrix} e^{\gamma_n^0 z} \quad z < 0 \quad (16)$$

$$\sum_{m=-\infty}^{\infty} f_m \begin{pmatrix} \mathbf{E}_m \\ \mathbf{H}_m \end{pmatrix} e^{\gamma_m z} \quad 0 < z < d \quad (17)$$

$$\sum_{n=-N}^N B_n \begin{pmatrix} \mathbf{E}_n^0 \\ \mathbf{H}_n^0 \end{pmatrix} e^{\gamma_n^0(z-d)} + \sum_{n > N} B_n \begin{pmatrix} \mathbf{E}_n^0 \\ \mathbf{H}_n^0 \end{pmatrix} e^{\gamma_n^0(z-d)} \quad d < z \quad (18)$$

where superscript ‘0’ denotes modes and propagation constants in the surrounding lossless medium M_0 . Although not explicitly noted, the enumeration excludes the cases $n = 0$ and $m = 0$, since there are no modes corresponding to these indices (as previously mentioned). We have explicitly splitted the modes in the surrounding waveguide in propagating and evanescent waves, denoting the number of propagating modes by N . Note that the reference plane for the B coefficients is chosen to be the right boundary through the shift $z \rightarrow z - d$ in the exponentials.

The boundary conditions are that the tangential \mathbf{E} and \mathbf{H} fields should be continuous. This is ensured by the following procedure. Fix $z = 0$ in expansions (16) and (17), multiply each expansion with $\begin{pmatrix} -\hat{z} \times \mathbf{H}_n^0 \\ \hat{z} \times \mathbf{E}_n^0 \end{pmatrix}^H$, and integrate over the cross section. We use the notation

$$P'_{mn} = \frac{1}{2} \int_{\Omega} \hat{z} \cdot \left(\mathbf{E}_m \times (\mathbf{H}_n^0)^* + (\mathbf{E}_n^0)^* \times \mathbf{H}_m \right) dS \quad (19)$$

for the product between expansion functions in different parts of the waveguide. If the cross sections of the different parts are different, this integral should be understood in terms of the common part of the cross section, and another set of equations is generated by the condition that the total tangential electric field on the metallic non-aperture part of the junction should be zero. We do not give the details of this procedure since it does not change the overall results. Making use of the quasi-orthogonality relations (13) in the surrounding lossless medium, we obtain the following equations (remember that for evanescent waves $P_{nm} = 0$, but the combination P_{-nm} may be nonzero)

$$A_n P_{nn} = \sum_{m=-\infty}^{\infty} f_m P'_{mn} \quad 1 \leq n \leq N \quad (20)$$

$$A_n P_{nn} = \sum_{m=-\infty}^{\infty} f_m P'_{mn} \quad -N \leq n \leq 1 \quad (21)$$

$$A_{-n} P_{-nn} = \sum_{m=-\infty}^{\infty} f_m P'_{mn} \quad N < n \quad (22)$$

$$0 = \sum_{m=-\infty}^{\infty} f_m P'_{mn} \quad n < -N \quad (23)$$

with similar equations for the B -coefficients. In the forward scattering problem, the coefficients of the incident waves, $\{A_n\}_{n=1}^N$ and $\{B_{-n}\}_{n=1}^N$, are known, and the remaining coefficients are to be determined assuming full knowledge of the modes inside and outside the MUT. Equation (23) and the corresponding equation

$$0 = \sum_{m=-\infty}^{\infty} f_m e^{\gamma_m d} P'_{mn} \quad N < n \quad (24)$$

for the opposite side describe the absence of incident evanescent waves on either side of the MUT. Based on the reasoning that these equations span all degrees of freedom except the $2N$ propagating modes in the surrounding medium, we assume that they can be used to eliminate all of the modes in the material except $2N$ ones, i.e., all higher order expansion coefficients $\{f_m\}_{|m|>N}$ can be expressed in terms of $\{f_m\}_{m=-N}^N$. This means Equation (20) and the corresponding equation for the $\{B_{-n}\}_{n=1}^N$ coefficients represent two $N \times 2N$ systems of linear equations, from which $\{f_m\}_{m=-N}^N$ can be determined from $\{A_n, B_{-n}\}_{n=1}^N$. The coefficients $\{f_m\}_{m=-N}^N$ can then be inserted in (21)

and (22) (and the corresponding equations for the B -coefficients) to give the coefficients of the scattered field. Considering only the propagating modes in the surrounding medium, this corresponds to a matrix equation

$$\{A_{-n}, B_n\}_{n=1}^N = S\{A_n, B_{-n}\}_{n=1}^N \quad (25)$$

where S is a $2N \times 2N$ matrix. Any linear scattering problem can be represented in this way, and this section has provided an outline to how the S -matrix can be computed, although it may in practice be very difficult to find closed form expressions for it. In the two-port network case ($N = 1$), this matrix can be measured with a network analyzer.

6. THE INVERSE SCATTERING PROBLEM

In the inverse scattering problem the aim is to infer information of the scattering system from scattering data. In our case, the ultimate goal is to determine the material matrix M from reflection and transmission coefficients, corresponding to the S -matrix in (25). To solve this problem completely is indeed a challenge, but we can at least obtain partial information on the wave propagation characteristics.

Assume that in the full problem, the interfaces are so widely separated that only the first M modes in the MUT contribute to the coupling between the interfaces. At the left interface, Equation (23) can then be written

$$\sum_{m=M+1}^{\infty} f_m P'_{mn} = - \sum_{m=-M}^M f_m P'_{mn} \quad (26)$$

the key point being that in the left hand side there are only ‘plus’ modes, hence these can be determined as functions of $\{f_m\}_{m=-M}^M$ not depending on the sample length d . A corresponding equation exists for the right interface, where instead only the higher order ‘minus’ modes occur. The interpretation of this is that the higher order modes, i.e., the evanescent modes in the material, only exist around the interfaces. This means Equations (20) and (21) can be represented as the matrix equation

$$\{A_n\}_{n=-N}^N = K_1 \{f_m\}_{m=-M}^M \quad (27)$$

where the $2N \times 2M$ coupling matrix K_1 does not depend on the sample length d . The corresponding equation for the right interface is

$$\{f_m e^{\gamma_m d}\}_{m=-M}^M = K_2 \{B_n\}_{n=-N}^N \quad (28)$$

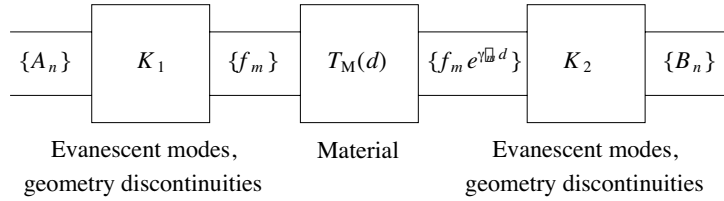


Figure 3. A box representation of the scattering situation. The coupling matrices K_1 and K_2 connect the propagating modes inside the material to the propagating modes in the surrounding medium, and the transmission matrix $T_M(d)$ models the propagation inside the material. The total transmission matrix from right to left, taking into account the possible mismatch at the material boundaries, is the product $T(d) = K_1 T_M(d) K_2$.

where the $2M \times 2N$ coupling matrix K_2 does not depend on d . Since we have

$$\{f_m\}_{m=-M}^M = \text{diag}\left(e^{-\gamma_m d}\right) \{f_m e^{\gamma_m d}\}_{m=-M}^M = T_M(d) \{f_m e^{\gamma_m d}\}_{m=-M}^M \quad (29)$$

where $\text{diag}(e^{-\gamma_m d})$ denotes a $2M \times 2M$ diagonal matrix with the propagation factors $e^{-\gamma_m d}$ on the diagonal, we obtain the full transmission matrix as the product

$$\{A_n\}_{n=-N}^N = K_1 T_M(d) K_2 \{B_n\}_{n=-N}^N = T(d) \{B_n\}_{n=-N}^N \quad (30)$$

where the only dependence on the sample length d is via the diagonal matrix $T_M(d)$. The situation is depicted in Figure 3.

So far, we have not touched upon the subject of the relation between M and N , i.e., the number of propagating modes in the material and the surrounding medium, respectively. For the inverse problem to be well posed, we require that the scattering situation can be arranged so that $M \leq N$ (this can be done by controlling the cut-off frequencies via the geometry, see Section 7). This is based on the reasoning that each propagating mode represents a degree of freedom, and in order to determine M degrees of freedom inside the material, we need to be able to control at least as many degrees of freedom outside the material.

The T -matrix is not directly accessible from measurement data, but the S -matrix in (25) can be deduced by varying the input coefficients $\{A_n, B_{-n}\}_{n=1}^N$ and measuring the response coefficients

$\{A_{-n}, B_n\}_{n=1}^N$. The T -matrix is then found by rearranging the S -matrix to obtain the mapping $\{B_n, B_{-n}\}_{n=1}^N \rightarrow \{A_n, A_{-n}\}_{n=1}^N$. An example of this procedure for the single-mode case is given in Section 7.

Performing this procedure for two different sample lengths d_1 and d_2 , we can determine two matrices $T(d_1)$ and $T(d_2)$. We assume that $M = N$ and that all matrices are invertible. We find

$$T(d_2)^{-1}T(d_1) = K_2^{-1}T_M(d_2)^{-1}T_M(d_1)K_2 = K_2^{-1}T_M(d_1 - d_2)K_2 \quad (31)$$

where we made use of the diagonal representation of the matrix $T_M(d)$ in (29). This new matrix is a similarity transformation of the matrix $T_M(d_1 - d_2)$, which has eigenvalues $\{e^{-\gamma_m(d_1-d_2)}\}_{m=-N}^N$. Thus, the matrix $T(d_2)^{-1}T(d_1)$ has the same eigenvalues, and with knowledge of the two lengths d_1 and d_2 the propagation constants γ_m can be determined.

The same procedure can be applied to the matrix $T(d_1)T(d_2)^{-1} = K_1T_M(d_1 - d_2)K_1^{-1}$. The eigenvectors can also be extracted and used to find the matrices K_1 and K_2 , however, it remains an open problem how to utilize this information in order to obtain more data on the material.

We finally note that the reference plane for the measurement does not need to be at the material boundary. This is due to the fact that a shift of reference plane in a lossless waveguide simply corresponds to $T \rightarrow UTV^H$, where U and V are unitary matrices. This means

$$T(d_2)^{-1}T(d_1) \rightarrow VT(d_2)^{-1}U^HUT(d_1)V^H = VT(d_2)^{-1}T(d_1)V^H \quad (32)$$

which does not change the eigenvalues, only the eigenvectors. Thus, if we are only interested in the propagation constants, the reference plane on each side of the sample is arbitrary as long as it is the same for both samples. But if we want information related to the eigenvectors, it is necessary to calibrate the reference plane to be at the material boundary.

The same reasoning also applies to the circumstance that if the equipment is not calibrated, we do not really measure the mode coefficient, but rather how this mode couples to a probe and is fed back in a cable; such circumstances are modeled by transformations of the form $T \rightarrow FTG^{-1}$, where F and G are matrices (or error boxes) modeling the probes at each end. Obviously, this does not change the situation compared to the previous paragraph.

7. NUMERICAL EXAMPLES

To illustrate the algorithm for the inverse scattering problem, we apply it to numerically simulated data. The algorithm determines



Figure 4. The geometry and mesh of the numerical examples. The two surrounding waveguides are designed for X-band operation (8.2–12.4 GHz, cutoff frequency 6.55 GHz), with cross section 2.29×1.02 cm and length 5.00 cm. Each open end is used as a port for the TE_{10} mode. A waveguide section of cross section 1.25×1.02 cm and length 4.00 cm or 5.00 cm is filled with the material under test. The mesh uses 3514 tetrahedral elements.

propagation constants, but in order to deduce material parameters from the propagation constants, it is necessary to have an explicit relation between them. The examples in this section are chosen among the very few such results that can be found in the literature. The results in this section can be transformed to other frequency regions by simultaneously scaling the dimensions of the waveguide and the frequency.

The waveguide setup is shown in Figure 4. The center part of the waveguide, containing the MUT, has different physical dimensions from the surrounding waveguides. This is in order to limit the number of propagating modes in the MUT, and achieve the condition $M = N$. We need two central waveguide sections with different lengths, corresponding to the different lengths of the material samples. The simulations were made with the program Comsol Multiphysics version 3.3, which is based on the Finite Element Method. Note that this means the forward problem generating the data for the inverse problem is not the mode-matching formulation in Section 5, but rather a numerical method for general problems.

The cutoff frequency for the TE_{10} mode of the air-filled waveguides is 6.55 GHz, and the frequency interval for simulation was chosen as 7–15 GHz. In a first test, the central waveguide part was filled with a non-magnetic isotropic material with relative permittivity $\epsilon_r = 4$ and conductivity $\sigma = 0.1$ S/m, implying a dispersive complex relative permittivity $\epsilon(\omega) = \epsilon_r + \frac{\sigma}{i\omega\epsilon_0}$, where ϵ_0 is the permittivity of vacuum. The calculations were made for the two lengths $d_1 = 4.00$ cm and $d_2 = 5.00$ cm. The program generates S -parameters for the structure with reference planes at the ports, where the S -parameters are defined from

$$\begin{pmatrix} A_{-1} \\ B_1 \end{pmatrix} = \begin{pmatrix} S_{11} & S_{12} \\ S_{21} & S_{22} \end{pmatrix} \begin{pmatrix} A_1 \\ B_{-1} \end{pmatrix} \quad (33)$$

However, we want to use the relation

$$\begin{pmatrix} A_1 \\ A_{-1} \end{pmatrix} = \begin{pmatrix} T_{11} & T_{12} \\ T_{21} & T_{22} \end{pmatrix} \begin{pmatrix} B_1 \\ B_{-1} \end{pmatrix} \quad (34)$$

in the algorithm determining the propagation constants. The relations between these parameters are [13]

$$T_{11} = 1/S_{21} \quad (35)$$

$$T_{12} = -S_{22}/S_{21} \quad (36)$$

$$T_{21} = S_{11}/S_{21} \quad (37)$$

$$T_{22} = (S_{12}S_{21} - S_{11}S_{22})/S_{21} \quad (38)$$

After using this transformation, we can find the propagation constants from the eigenvalues of the matrix $T(d_2)^{-1}T(d_1)$. In this procedure, it is necessary to unwrap the phase (remove discontinuities $\geq \pi$ in the imaginary part) in order to avoid discontinuities in the propagation constants as functions of ω . The complex permittivity is then determined by inverting the relation $\beta^2 = \epsilon(\omega)\omega^2/c_0^2 - \lambda$, where $\lambda = (\pi/a)^2$, with a being the width of the center waveguide. The resulting quantity is plotted in Figure 5. The code doing this procedure on given S -parameter data is only a few ten lines in Matlab.

It is seen that the method can determine the complex permittivity rather accurately. The errors can be attributed to the numerical accuracy of the FEM program generating the data. A full-blown stability analysis of the algorithm is beyond the scope of this paper, and we settle for the following simple numerical test. We perturbed the S -parameters from the simulations by adding noise generated by the Matlab command `randn` multiplied by three different factors 0.1, 0.01, and 0.001, representing different noise levels. The relative error in the calculated permittivity was of the same order as the perturbation in all these cases, demonstrating that the algorithm is reasonably stable.

To extend the results, we turn to the anisotropic case. A non-magnetic, anisotropic dielectric material with its principal axes aligned with the walls of a rectangular waveguide is described by the permittivity

$$\epsilon = \epsilon_0 \begin{pmatrix} \epsilon_x & 0 & 0 \\ 0 & \epsilon_y & 0 \\ 0 & 0 & \epsilon_z \end{pmatrix} \quad (39)$$

where ϵ_0 is the permittivity of vacuum and the coordinates are the natural ones in a rectangular waveguide. It is shown in [10] that the same dispersion relation applies for the fundamental TE mode for this

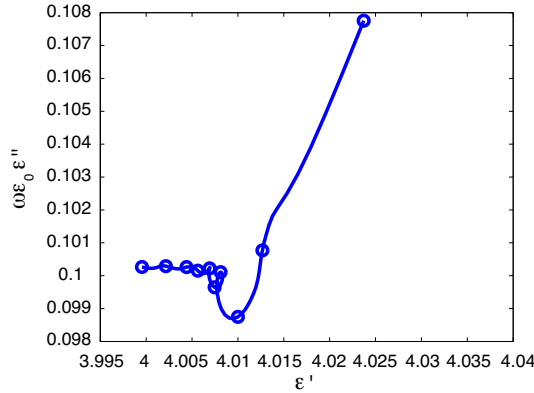


Figure 5. The complex permittivity computed from the S -parameters by the algorithm in this paper. The circles indicate 10 linearly distributed frequencies in the interval 7–15 GHz, smallest frequencies farthest to the left. Notice that the imaginary part (the y -axis) is scaled by the factor $\omega\epsilon_0$, making it correspond to the conductivity σ . Also observe the tight scales. The relatively large deviation for high frequencies is probably due to multimode propagation.

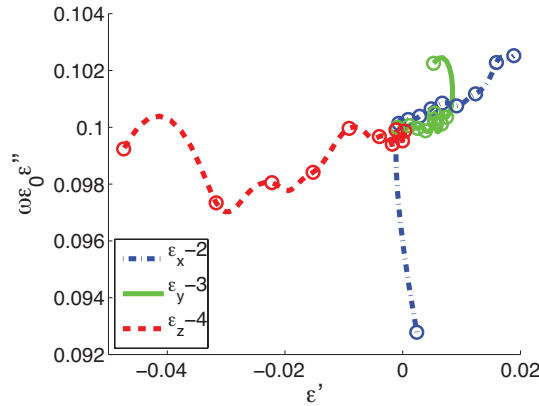


Figure 6. Results for an anisotropic material. In this case, the narrow section of the waveguide has principal values $\epsilon_x = 2 + i\sigma/(\omega\epsilon_0)$, $\epsilon_y = 3 + i\sigma/(\omega\epsilon_0)$, and $\epsilon_z = 4 + i\sigma/(\omega\epsilon_0)$, where $\sigma = 0.1\text{ S/m}$. The mesh and the frequency range, 7–15 GHz, are the same as in the other examples, and the errors are largest for higher frequencies. The curve for $\epsilon_x - 2$ starts off with a relatively large error at around $(0.0024, 0.0928)$ for $f = 7\text{ GHz}$ in the figure. This is due to that for this principal value the midsection waveguide is then operating below its cutoff frequency, which is 8.5 GHz.

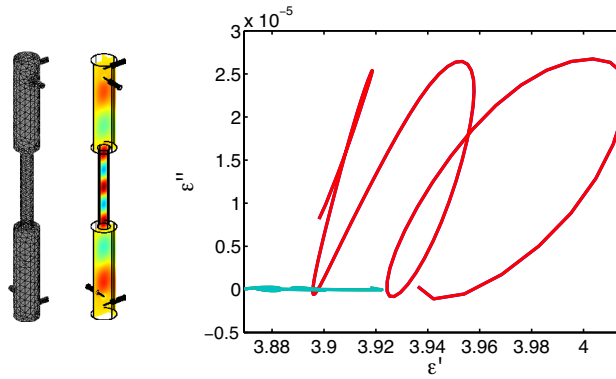


Figure 7. Reconstructing an isotropic material in a circular waveguide, where the air part has radius 2.5 cm and the MUT part has radius 1.25 cm, resulting in two propagating TE_{11} modes in the frequency range $3.6 \text{ GHz} \leq f \leq 4.6 \text{ GHz}$. The MUT is lossless, with $\epsilon_r = 4$. The ends of the circular waveguides are terminated by PEC surfaces, and the four ports are defined in the coaxial cables. The two curves correspond to different eigenvalues/propagation factors. Note the very small numbers on the y -axis.

material as for an isotropic material, i.e., $\gamma^2 = \lambda - \omega^2 \epsilon_{x,y,z} \epsilon_0 \mu_0$. In order to deduce all three principal values, the material sample is rotated so that each principal direction is aligned with the polarization of the fundamental TE mode in the waveguide. The results are very accurate, and are given in Figure 6.

To conclude this section and demonstrate that the algorithm holds also in the multiport setting, we present a case where $M = N = 2$. This is realized in a circular waveguide geometry as in Figure 7, where the circular waveguide is fed by four pins, two on each side of the MUT, with the ports defined in the coaxial cables. The error is larger in this case than for the rectangular waveguide, which can be attributed to a poor resolution of the fine structure in the coaxial cables.

8. CONCLUSIONS

In this paper, we have analyzed the forward and inverse scattering problems of a bianisotropic material sample in a metallic waveguide. Under the assumption that there are as many modes inside the MUT as outside, measurements on two samples with different lengths are enough to determine the propagation constants inside the MUT.

Additional information on the modes is available, but the utilization of this information remains a problem for further research.

Since the algorithm primarily determines propagation constants and not material data, it is necessary to have a precise characterization of the mode problem (6) in order to extract material data. This is possible for a few special cases, especially isotropic media in waveguides with arbitrary cross section and anisotropic media in rectangular waveguides, where there is an explicit expression connecting the propagation constant to frequency and material data. To extend the results to more general materials, a more detailed investigation of the mode problem is necessary.

The analysis leading to the determination of propagation constants is very general, and holds for any linear material. For instance, nothing in the analysis changes if the material is heterogeneous in the (x, y) -plane, but does not depend on the z variable. Indeed, this has been utilized in the numerical example in Section 7, where we used a different cross section of the waveguide containing the sample. Actually, the analysis is applicable to any structure in which the electromagnetic field can be described by an expansion in propagating and evanescent modes. In particular, this includes Bloch waves in periodic structures.

There is probably a large range of special cases where the proposed formalism reduces significantly in complexity. Most prominently, in waveguides filled with isotropic materials, there is almost no coupling between different modes. Also, there are significant simplifications for materials where an optical axis is along the waveguide axis.

The major assumption in this paper is that the number of propagating modes is the same inside and outside the MUT, or possibly a smaller number inside the MUT. The main reason for this assumption is that it is necessary to be able to explore the degrees of freedom available *inside* the material by varying the degrees of freedom *outside* the material. This is not always easy to achieve: if the surrounding medium is air, the cutoff frequencies inside the MUT are usually lower, implying that there may be more propagating modes inside the material. In order to achieve the same number of propagating modes, we may choose the surrounding material parameters M_0 to obtain a small contrast to the MUT parameters M , or place the MUT in a somewhat narrower waveguide than its surrounding material. The latter strategy was employed in Section 7 of this paper.

ACKNOWLEDGMENT

The work reported in this paper was supported by the Swedish Research Council. The author acknowledges many fruitful discussions regarding this paper with Professor Gerhard Kristensson, Professor Anders Karlsson, Docent Mats Gustafsson, Professor Anders Melin, and Doctor Andreas Ioannidis, all at the Department of Electrical and Information Technology at Lund University, Sweden.

REFERENCES

1. Akhtar, M. J., L. E. Fehrer, and M. Thumm, "A waveguide-based two-step approach for measuring complex permittivity tensor of uniaxial composite materials," *IEEE Trans. Microwave Theory Tech.*, Vol. 54, No. 5, 2011–2022, May 2006.
2. Baker-Jarvis, J., R. G. Geyer, J. John H. Grosvenor, M. D. Janezic, C. A. Jones, B. Riddle, and C. M. Weil, "Dielectric characterization of low-loss materials: A comparison of techniques," *IEEE Transactions on Dielectrics and Electrical Insulation*, Vol. 5, No. 4, 571–577, Aug. 1998.
3. Baker-Jarvis, J., E. J. Vanzura, and W. A. Kissick, "Improved technique for determining complex permittivity with the transmission/reflection method," *IEEE Trans. Microwave Theory Tech.*, Vol. 38, No. 8, 1096–1103, Aug. 1990.
4. Barybin, A. A., "Modal expansions and orthogonal complements in the theory of complex media waveguide excitation by external sources for isotropic, anisotropic, and bianisotropic media," *Progress In Electromagnetics Research*, PIER 19, 241–300, 1998.
5. Bresler, A. D., "The far fields excited by a point source in a passive dissipationless anisotropic uniform waveguide," *IRE Trans. on Microwave Theory and Techniques*, Vol. 7, No. 2, 282–287, Apr. 1959.
6. Bresler, A. D., "On the discontinuity problem at the input to an anisotropic waveguide," *IRE Trans. on Antennas and Propagation*, Vol. 7, No. 5, 261–272, Dec. 1959.
7. Bresler, A. D., "Vector formulations for the field equations in anisotropic waveguides," *IRE Trans. on Microwave Theory and Techniques*, Vol. 7, No. 2, 298, Apr. 1959.
8. Bresler, A. D., G. H. Joshi, and N. Marcuvitz, "Orthogonality properties for modes in passive and active uniform wave guides," *J. Appl. Phys.*, Vol. 29, No. 5, 794–799, May 1958.
9. Busse, G., J. Reinert, and A. F. Jacob, "Waveguide characteri-

- zation of chiral material: Experiments,” *IEEE Trans. Microwave Theory Tech.*, Vol. 47, No. 3, 297–301, 1999.
10. Damaskos, N. J., R. B. Mack, A. L. Maffett, W. Parmon, and P. L. E. Uslenghi, “The inverse problem for biaxial materials,” *IEEE Trans. Microwave Theory Tech.*, Vol. 32, No. 4, 400–405, Apr. 1984.
 11. De Hoop, A. T., *Handbook of Radiation and Scattering of Waves*, Academic Press, San Diego, 1995.
 12. Deshpande, M. D., C. J. Reddy, P. I. Tiemsin, and R. Cravey, “A new approach to estimate complex permittivity of dielectric materials at microwave frequencies using waveguide measurements,” *IEEE Trans. Microwave Theory Tech.*, Vol. 45, No. 3, 359–366, Mar. 1997.
 13. Frickey, D. A., “Conversions between S , Z , Y , h , $ABCD$, and T parameters which are valid for complex source and load impedance,” *IEEE Trans. Microwave Theory Tech.*, Vol. 42, No. 2, 205–211, Feb. 1994.
 14. Gustafsson, M., *Wave Splitting in Direct and Inverse Scattering Problems*, PhD thesis, Lund Institute of Technology, Department of Electromagnetic Theory, P. O. Box 118, S-221 00 Lund, Sweden, 2000. <http://www.eit.lth.se+>.
 15. Quéffélec, P., M. L. Floc’h, and P. Gelin, “Nonreciprocal cell for the broad-band measurement of tensorial permeability of magnetized ferrites: Direct problem,” *IEEE Trans. Microwave Theory Tech.*, Vol. 47, No. 4, 390–397, Aug. 1999.
 16. Quéffélec, P., M. L. Floc’h, and P. Gelin, “New method for determining the permeability tensor of magnetized ferrites in a wide frequency range,” *IEEE Trans. Microwave Theory Tech.*, Vol. 48, No. 8, 1344–1351, Aug. 2000.
 17. Reinert, J., G. Busse, and A. F. Jacob, “Waveguide characterization of chiral material: Theory,” *IEEE Trans. Microwave Theory Tech.*, Vol. 47, No. 3, 290–296, 1999.
 18. Sjöberg, D., “Homogenization of dispersive material parameters for Maxwell’s equations using a singular value decomposition,” *Multiscale Modeling and Simulation*, Vol. 4, No. 3, 760–789, 2005.
 19. Sjöberg, D., C. Engström, G. Kristensson, D. J. N. Wall, and N. Wellander, “A Floquet-Bloch decomposition of Maxwell’s equations, applied to homogenization,” *Multiscale Modeling and Simulation*, Vol. 4, No. 1, 149–171, 2005.
 20. Wolfson, B. J. and S. M. Wentworth, “Complex permittivity and permeability measurement using a rectangular waveguide,”

- Microwave Opt. Techn. Lett.*, Vol. 27, No. 3, 180–182, Nov. 2000.
21. Wu, X., “A linear-operator formalism for bianisotropic waveguides,” *Int. J. Infrared and MM Waves*, Vol. 16, No. 2, 419–434, 1995.
 22. Xu, Y. and R. G. Bosisio, “An efficient method for study of general bi-anisotropic waveguides,” *IEEE Trans. Microwave Theory Tech.*, Vol. 43, No. 4, 873–879, Apr. 1995.
 23. Xu, Y. and R. G. Bosisio, “A study on the solutions of chirowaveguides and bianisotropic waveguides with the use of coupled-mode analysis,” *Microwave Opt. Techn. Lett.*, Vol. 14, No. 5, 308–311, Apr. 1997.